Available online at www.sciencedirect.com
ScienceDirect
JOURNAL OF RARE EARTHS, Vol. 33, No. 3, Mar. 2015, P. 227
JOURNAL OF RARE EARTHS
www.re-journal.com/en/

Effect of Yb^{3+} concentration on upconversion luminescence of AlON:Er^{3+} phosphors

SU Mingyi (苏明毅)[1,2], ZHOU Youfu (周有福)[1,*], WANG Kun (王 坤)[1,2], HUANG Decai (黄得财)[1], XU Wentao (许文涛)[1], CAO Yongge (曹永革)[1]

(1. Key Laboratory of Optoelectronic Materials Chemistry and Physics, Fujian Institute of Research on the Structure of Matter, Chinese Academy of Sciences, Fuzhou 350002, China; 2. University of Chinese Academy of Sciences, Beijing 100039, China)

Received 28 May 2014; revised 11 December 2014

Abstract: AlON:1.6 mol.%Er^{3+}, *x* mol.%Yb^{3+} (*x*=0, 2.6, 3.1, 3.6, 4.1, 4.6) phosphors were synthesized successfully by aluminothermic reduction and nitridation (ATRN) method and characterized by X-ray diffraction (XRD), scanning electron microscopy (FESEM) and upconversion photoluminescence (UCPL) emission spectra. Under the excitation of diode laser 980 nm, the green (556 nm) and red (655 nm) upconverted emissions were observed, attributed to the $^4S_{3/2}\rightarrow{}^4I_{15/2}$ and $^4F_{9/2}\rightarrow{}^4I_{15/2}$ transition of Er^{3+} respectively. The emission intensity increased with increasing Yb^{3+} concentration due to the energy transfer (ET) between Yb^{3+} and Er^{3+}. The upconverted emission reached the highest as *x*=3.6, and was pump-power dependent involving a two-photon process.

Keywords: AlON; phosphor; upconversion luminescence; energy transfer; rare earths

As green energy materials, upconversion photoluminescence (UCPL) phosphors have attracted much attention due to their potential applications in solid state lasers, displays and biological fluorescence devices[1–5]. Rare earth (RE) ions, such as Er^{3+}, Tm^{3+}, Ho^{3+} and Pr^{3+}, have been commonly used as activator[6–9]. Meanwhile, Yb^{3+} ion has been used as an efficient sensitizer due to the large absorption cross section at 980 nm and further energy transfer to activator[10–13].

To weaken the possibility of nonradiative transitions, the host materials should have low phonon energy. With cubic spinel structure, aluminum oxynitride (AlON) exhibits interesting mechanical, optical and photoluminescent properties[14–16]. As UCPL phosphor, AlON doped with Er^{3+}, co-doped with Er^{3+} and Mg^{2+}, co-doped with Yb^{3+} and Tm^{3+} have been reported respectively[17–19]. The adopted approach was the two-step route: the AlON powder was synthesized by carbothermal reduction and nitridation (CTRN) firstly, and then mixed corresponding RE and sintered. The two-step approach has its drawbacks: complexity and potential inhomogeneity. Thus, the one-step route that simplifies the production technology as well as reduces the cost is critical importance. Besides the CTRN, AlON can also be prepared by the aluminothermic reduction and nitridation (ATRN) method. Furthermore, ATRN method can avoid the possible residual of carbon by CTRN[20,21]. If the ATRN method could be introduced into the one-step route, high quality AlON phosphors are expected to be obtained with simplicity and cost-effectiveness.

Herein, a series of Er^{3+}-Yb^{3+} codoped AlON phosphors were synthesized successfully by ATRN method for the first time. To demonstrate the sensibilization of Yb^{3+}, low concentration of Er^{3+} (1.6 mol.%) was introduced. The UCPL spectra with different Yb^{3+} concentrations were presented, along with the dependence of emission intensity upon pump power to investigate the UCPL mechanism.

1 Experimental

1.1 Preparation

The starting materials were commercially available and used without further purification, involving α-Al_2O_3 (99.9%, 30 nm) and Al (99.95%, 1–2 μm), Er_2O_3 (99.99%) and Yb_2O_3 (99.99%). The amount of α-Al_2O_3 and Al was weighed based on AlON with 27 mol.%. Er_2O_3 and Yb_2O_3 were worked out with 1.6 mol.% Er^{3+} and *x* mol.% Yb^{3+} (*x*=0, 2.6, 3.1, 3.6, 4.1, 4.6), respectively. All of the materials were mixed thoroughly in alcohol media and dried at 80 °C for 3 h in a vacuum drying oven. The homogeneous mixture was put into a BN crucible and calcined at 1550 °C for 1.5 h, then at 1750 °C for 2.5 h un-

Foundation item: Project supported by National Natural Science Foundation of China (91022035), "One Hundred Talent Project", and the Natural Science Foundation of Fujian Province (2014H0055)

* **Corresponding author:** ZHOU Youfu (**E-mail:** yfzhou@fjirsm.ac.cn; **Tel.:** +86-591-63179089)

DOI: 10.1016/S1002-0721(14)60407-5

der flowing N_2 atmosphere, obtaining Er, Yb co-doped AlON product.

1.2 Characterization

Phase identification was carried out by an X-ray diffractometer (Japan Rigaku SCXmini) using Cu Kα radiation (λ=0.15406 nm) operated at 30 kV and 10 mA. The FESEM images were obtained with a JSM-6700F (JEOL) field-emission-type microscope with operation voltage in the range of 0.5–30 kV to observe the morphology. The UCPL emission spectra were measured with a Horiba JY Fluorolog-3 spectrometer at room temperature.

2 Results and discussion

Fig. 1 shows the XRD patterns of AlON powders doped with 1.6 mol.% Er^{3+} and different Yb^{3+} concentrations. For the specimens of Yb^{3+} concentration below 3.6 mol.%, the spectra can be attributed to spinel-type AlON (JCPDS No. 80-2172) without any impurity. In addition, the peaks are sharp and intense due to good crystalline. It is noteworthy that small amount $YbAlO_3$ (JCPDS No. 48-1633) appears for the specimens with higher Yb^{3+} concentrations (x>3.6). It is well-known that impure phase is negative to prepare high transparent ceramic. Thus, only the UCPL properties of the specimens with x≤3.6 are presented.

Fig. 2 shows the SEM images of pure AlON, solely doped AlON:1.6 mol.%Er^{3+}, and co-doped AlON:1.6 mol.%Er^{3+} and different Yb^{3+} concentrations. All of the specimens display irregular morphology. It is interesting that the average particle sizes of AlON and AlON:1.6 mol.%Er^{3+} are 2.1 and 2.4 μm respectively, while those of the codoped samples increase dramatically with the introduction of Yb^{3+} ions (above 10 μm). This phenomenon is attributed to the increase amount of transient liquid phases with Yb_2O_3 doped, resulting in accelerating the dissolution, diffusion, and precipitation processes[22].

Fig. 3 depicts the emission spectra of the phosphors under the excitation of λ_{ex}=980 nm of diode laser, showing Yb^{3+}-concentration dependence of the emission intensities. The green emission band is ranging from 519 to 566 nm, while the red one is stronger within the range of 640–695 nm. These emission bands are attributed to ($^2H_{11/2}$, $^4S_{3/2}$)→$^4I_{15/2}$ and $^4F_{9/2}$→$^4I_{15/2}$ transitions of Er^{3+} respectively. The UCPL processes of RE doping systems have been widely investigated. For the solely doped Er^{3+} system, the possible mechanism for the population of

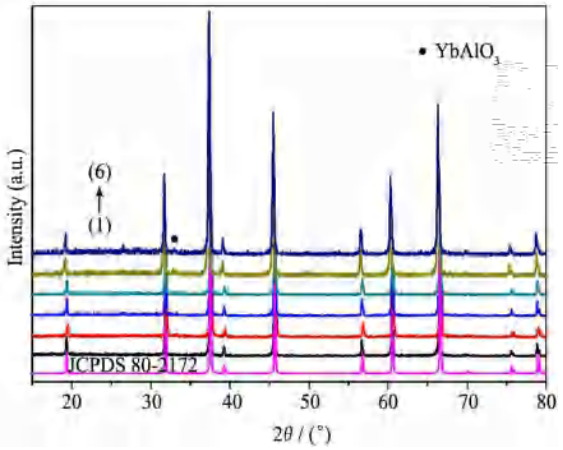

Fig. 1 Powder X-ray diffraction patterns of AlON:1.6Er^{3+},$x$$Yb^{3+}$ samples with x=0 mol.% (1), 2.6 mol.% (2), 3.1 mol.% (3), 3.6 mol.% (4), 4.1 mol.% (5) and 4.6 mol.% (6), respectively

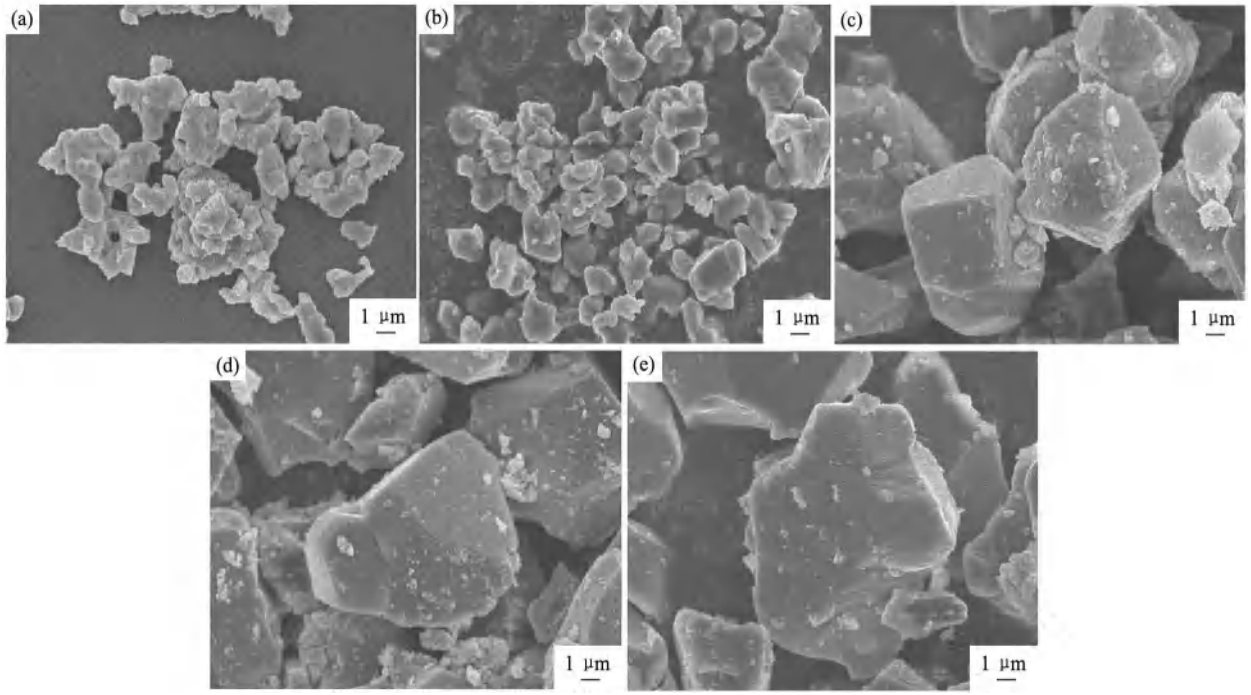

Fig. 2 SEM images of undoped AlON (a), AlON:1.6 mol.%Er^{3+} (b), AlON:1.6 mol.%Er^{3+}, 2.6 mol.%Yb^{3+} (c), AlON:1.6 mol.%Er^{3+}, 3.1 mol.%Yb^{3+} (d) and AlON:1.6 mol.%Er^{3+}, 3.6 mol.%Yb^{3+} (e)

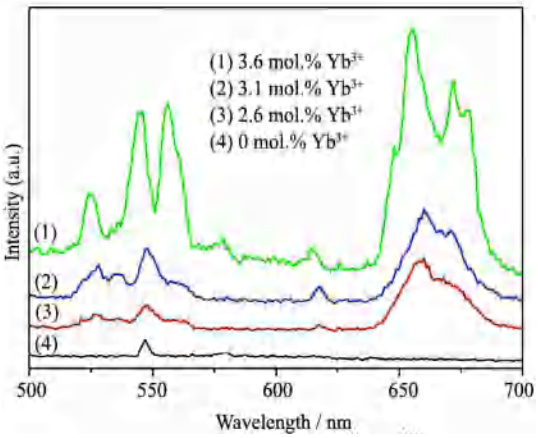

Fig. 3 Emission spectra of AlON:1.6Er^{3+},xYb^{3+} samples (x=0 mol.%, 2.6 mol.%, 3.1 mol.% and 3.6 mol.%)

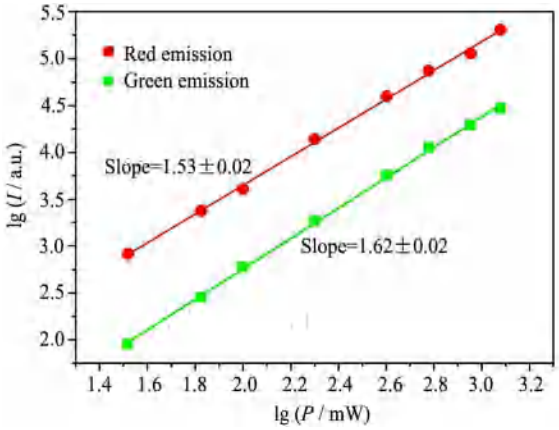

Fig. 4 Pump power dependce of UCPL of AlON:1.6Er^{3+},3.6Yb^{3+} composite phosphor

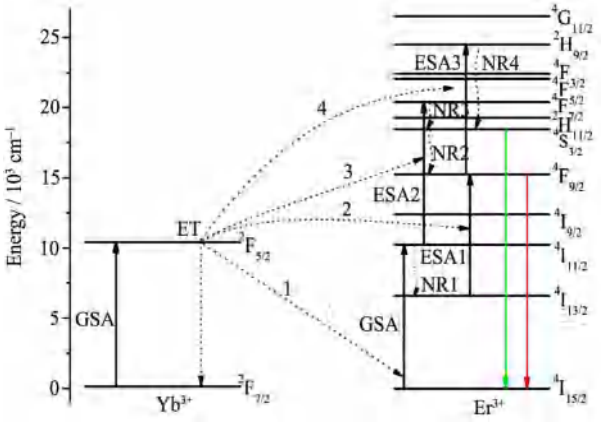

Fig. 5 Energy level diagram of Er^{3+} and Yb^{3+} ions and the proposed upconversion processes under the excitation of λ_{ex}= 980 nm

$^4I_{13/2}$ level (Fig. 5) is the cross-relaxation (CR) process: $^2H_{11/2}\rightarrow{}^4I_{9/2}$:$^4I_{15/2}\rightarrow{}^4I_{13/2}$. The distance between Er^{3+} ions will affect the CR rate. Thus, the red emission band is almost negligible for AlON:1.6 mol.%Er^{3+} [18].

For the Er^{3+} and Yb^{3+} co-doped system, Yb^{3+} ion has a considerably larger absorption cross section relative to that of Er^{3+}. Thus, Yb^{3+} ions absorb energy from 980 nm excitation firstly and then transfer to Er^{3+} ions. The energized Er^{3+} ions produce the radiative and the nonradiative transition further. These energy transfer processes strongly depend on the ion concentration. The intensity of the red and green emission increases slightly with increasing Yb^{3+} concentration initially, but increases dramatically as the Yb^{3+} concentration reaches 3.6 mol.% (Fig. 3). It is different from other systems, where the green emission decreases with increasing Yb^{3+} concentration[23–26]. Although the solubility of RE ion in AlON is poor[17,18], it seems that the codoped Yb^{3+} concentration with 3.6 mol.% in this system does not reach the quenching solubility leading to no decrease of the green emission.

To further understand the UCPL mechanism in AlON: 1.6 mol.%Er^{3+},3.6 mol.%Yb^{3+}, the pump power dependence of the UCPL intensities was conducted (Fig. 4). For the UCPL process, the upconverted emission intensities I_{UCPL} depends on the pump laser power I_p according to the following equation: $I_{UCPL}\propto I_p^n$, where n is the number of pumping photons absorbed per upconverted photon emitted[27]. From the experimental data, the n values for the red and the green upconverted emission band are 1.53 and 1.62, respectively. Larger n value for the green band indicates a faster growth of the green UCPL than the red UCPL with increasing pump power. Because both of n values are larger than 1.5, the red and the green upconverted emission bands originate from the two-photon process[23,28].

The typical energy level diagram of the UCPL for Er^{3+}, Yb^{3+} codoped system under 980 nm excitation is shown in Fig. 5. Usually, it can be treated as ground state absorption (GSA), excited state absorption (ESA), nonradiative process (NR) and energy transfer (ET). In general, upconversion occurs via successive ET processes from the Yb^{3+} to the Er^{3+} ion in the codoped system[10]. Following the GSA of the 980 nm photon, the Yb^{3+} ion is excited to the $^2F_{5/2}$ state. The Er^{3+} ion is excited to the intermediate excited state $^4I_{11/2}$ by energy transfer (ET1). By means of nonradiative processes (NR1), the Er^{3+} ions in the $^4I_{11/2}$ state relax to populate the $^4I_{13/2}$ states. Immediately following the interaction with another excited Yb^{3+} ion, the excited Er^{3+} ion is promoted to the $^4F_{9/2}$ state by ET2, and the red emission is succeeded. For the sample with Yb^{3+} doping less than 3.1 mol.%, ET3, ET4 and NR2 are difficult to occur, leading to slight change of red emission. The $^4S_{3/2}$ is the green emission state, the initial enhancement with increasing Yb^{3+} concentration can be assigned to the population of this state by ET3 and NR3.

With the Yb^{3+} concentration increasing continuously to 3.6 mol.%, the Er^{3+} ions are surrounded by more Yb^{3+} ions, resulting in easier energy transfer from ET1 to ET4 (a two-photon process). For the red emission, the population of the Er^{3+} ion at the $^4F_{9/2}$ state is via two processes:

$$^4I_{15/2}\xrightarrow{ET1}{}^4I_{11/2}\xrightarrow{NR1}{}^4I_{13/2}\xrightarrow{ET2}{}^4F_{9/2}$$

$$^4I_{11/2}\xrightarrow{ET3}{}^4F_{7/2}\xrightarrow{NR3}{}^4S_{3/2}\xrightarrow{NR2}{}^4F_{9/2}$$

For the green emission, the population of the Er^{3+} ion at

$^4S_{3/2}$ state can be produced by other two processes:

$$^4F_{9/2} \xrightarrow{ET4} {}^2H_{9/2} \xrightarrow{NR4} {}^4S_{3/2}$$

$$^4I_{11/2} \xrightarrow{ET3} {}^4F_{7/2} \xrightarrow{NR3} {}^4S_{3/2}$$

According to above processes, the ET3 and the ET4 significantly affect the intensity of the red and green emission. For higher Yb^{3+} concentration, facilitating ET3 and ET4 processes, is the principal reason for the sensibilization of UCPL in AlON:Er^{3+},Yb^{3+} system.

3 Conclusions

In summary, AlON co-doped with 1.6 mol.%Er^{3+} and different Yb^{3+} concentrations was synthesized by ATRN method. Under the 980 nm excitation, the green and red upconverted emissions were observed, which was pump-power dependent originating from the two-photon process. Combining the ET from Yb^{3+} to Er^{3+} with the ESA and the NR of Er^{3+}, the population of Er^{3+} ion at the $^4F_{9/2}$ state and the $^4S_{3/2}$ state increased evidently, resulting in a pronounced enhancement of the upconverted emissions for AlON:1.6 mol.%Er^{3+},3.6 mol.%Yb^{3+} phosphor.

References:

[1] Wang L Y, Li Y D. Controlled synthesis and luminescence of lanthanide doped $NaYF_4$ nanocrystals. *Chem. Mater.*, 2007, **19**(4): 727.

[2] Patra A, Friend C S, Kapoor R, Prasad P N. Fluorescence upconversion properties of Er^{3+}-doped TiO_2 and $BaTiO_3$ nanocrystallites. *Chem. Mater.*, 2003, **15**(19): 3650.

[3] Xu S Q, Ma H P, Fang D W, Zhang Z X, Jiang Z H. Tm^{3+}/Er^{3+}/Yb^{3+}-codoped oxyhalide tellurite glasses as materials for three-dimensional display. *Mater. Lett.*, 2005, **59**(24-25): 3066.

[4] Garrido-Hernández A, García-Murillo A, Carrillo-Romo F, Cruz-Santiago L A, Chadeyron G, Morales-Ramírez A, Velumani S. Structural studies of $BaTiO_3$:Er^{3+} and $BaTiO_3$:Yb^{3+} powders synthesized by hydrothermal method. *J. Rare Earths*, 2014, **32**(11): 1016.

[5] Ye Y S, Jiang Z H, Wang Q Z, Zhu Z S, Wang X, Sui Z L, Dai R C, Wang Z P, Zhang Z M, Ding Z J. Upconversion luminescence of $NaYF_4$:Yb,Er nanocrystals with high uniformity. *J. Rare Earths*, 2014, **32**(9): 802.

[6] Liu M, Wang S W, Tang D Y, Chen L D, Ma J. Preparation and upconversion luminescence of YAG($Y_3Al_5O_{12}$): Yb^{3+}, Ho^{3+} nanocrystals. *J. Rare Earths*, 2009, **27**(1): 66.

[7] Pecoraro E, Sousa D F, Lebullenger R, Hernandes A C, Nunes L A O. Evaluation of the energy transfer rate for the Yb^{3+}: Pr^{3+} system in lead fluoroindogallate glasses. *J. Appl. Phys.*, 1999, **86**(6): 3144.

[8] Pei X J, Hou Y B, Zhao S L, Xu Z, Teng F. Frequency upconversion of Tm^{3+} and Yb^{3+} codoped $YLiF_4$ synthesized by hydrothermal method. *Mater. Chem. Phys.*, 2005, **90**(2–3): 270.

[9] Liu M, Wang S W, Zhang J, An L Q, Chen L D. Preparation and upconversion luminescence of $Y_3Al_5O_{12}$:Yb^{3+}, Er^{3+} transparent ceramics. *J. Rare Earths*, 2006, **24**(6): 732.

[10] Vetrone F, Boyer J C, Capobianco J A, Speghini A, Bettinelli M. Effect of Yb^{3+} codoping on the upconversion emission in nanocrystalline Y_2O_3:Er^{3+}. *J. Phys. Chem. B*, 2003, **107**(5): 1107.

[11] Sun J Y, Xue B, Sun G C, Cui D P. Yellow upconversion luminescence in Ho^{3+}/Yb^{3+} co-doped $Gd_2Mo_3O_9$ phosphor. *J. Rare Earths*, 2013, **31**(8): 741.

[12] Dong Y M, Sun J, Yu W S, Li W H, Teng F. Preparation and properties of Nd,Yb:GGG polycrystalline nanopowders. *J. Adv. Ceram.*, 2012, **1**(4): 296.

[13] Lu L P, Zhang X Y. Optimization of synthesis of upconversion luminescence material $NaYF_4$:Er^{3+},Yb^{3+} nanometer-phosphor by low-temperature combustion synthesis method. *J. Rare Earths*, 2013, **31**(1): 8.

[14] Hartnett T M, Bernstein S D, Maguire E A, Tustison R W. Optical properties of ALON (aluminum oxynitride). *Infrared Phys. Technol.*, 1998, **39**(4): 203.

[15] Goldman L M, Balasubramanian S, Nagendra N, Smith M. ALON® optical ceramic transparencies for sensor and armor applications. *Structure*, 2012, **380**: 700.

[16] Wahl J M, Hartnett T M, Goldman L M, Twedt R, Warner C. Recent advances in AlON™ optical ceramic. *Proceedings of SPIE*, 2005, **5786**: 71.

[17] Zhang F, An L Q, Liu X J, Zhou G H, Yuan X Y, Wang S W. Upconversion luminescence in γ-AlON:Yb^{3+},Tm^{3+} ceramic phosphors. *J. Am. Ceram. Soc.*, 2009, **92**(8): 1888.

[18] Zhang F, Wang S W, Liu X J, An L Q, Yuan X Y. Upconversion luminescence in Er-doped γ-AlON ceramic phosphors. *J. Appl. Phys.*, 2009, **105**(9): 093542.

[19] Zhang F, Chen S, Zhang H L, Li J, Yang Y, Zhou G H, Liu X J, Wang S W. Upconversion luminescence of γ-AlON:Er^{3+} phosphors with Mg^{2+} Co-doping. *J. Am. Ceram. Soc.*, 2012, **95**(1): 27.

[20] Miao W F. Method for manufacturing aluminum oxynitride (AlON) powder and other nitrogen-containing powders. U.S. Patent: US 6955798, 2005.

[21] Zhou J C, Liao Z J, Qi J Q, Pang W, Wen Y, Wen J S, Wang H P, He J F, Wu D X, Lu T C. A new method for the preparation of transparent AlON ceramic. *Key Eng. Mater.*, 2008, **368**: 441.

[22] Ryu J H, Won H S, Park Y-G, Kim S H, Song W Y, Suzuki H, Yoon C-B, Kim D H, Park W J, Yoon C. Photoluminescence of Ce^{3+}-Activated β-SiAlON Blue Phosphor for UV-LED. *Electrochem. Solid-State Lett.*, 2010, **13**(2): H30.

[23] Vetrone F, Boyer J-C, Capobianco J A, Speghini A, Bettinelli M. Significance of Yb^{3+} concentration on the upconversion mechanisms in codoped Y_2O_3:Er^{3+},Yb^{3+} nanocrystals. *J. Appl. Phys.*, 2004, **96**(1): 661.

[24] Lu W L, Cheng L H, Sun J S, Zhong H Y, Li X P, Tian Y, Wan J, Zheng Y F, Huang L B, Yu T T, Yu H Q, Chen B J. The concentration effect of upconversion luminescence properties in Er^{3+}/Yb^{3+}-codoped $Y_2(MoO_4)_3$ phosphors. *Physica B*, 2010, **405**(16): 3284.

[25] Cao B S, He Y Y, Zhang L, Dong B. Upconversion properties of Er^{3+}-Yb^{3+}:$NaYF_4$ phosphors with a wide range of Yb^{3+} concentration. *J. Lumin.*, 2013, **135**(0): 128.

[26] Choi H Y, Kim J H, Park J Y, Moon B K, Jeong J H. Upconversion luminescence in Er/Yb codoped $Gd_3Al_5O_{12}$ phosphors. *J. Korean Phys. Soc.*, 2011, **59**(3): 2329.

[27] Pollnau M, Gamelin D R, Lüthi S R, Güdel H U, Hehlen M P. Power dependence of upconversion luminescence in lanthanide and transition-metal-ion systems. *Phys. Rev. B*, 2000, **61**(5): 3337.

[28] Wang W, Liu N, Du Y R, Wang Y J, Li L Y, Jiao H. Up-conversion luminescence properties of Yb^{3+}/Er^{3+} co-doped $AgGd(W,Mo)_2O_8$ phosphors. *J. Alloys Compd.*, 2013, **577**(0): 426.